LONG-TERM INDIRECT INDICES OF SOLAR VARIABILITY

JÜRG BEER (beer@eawag.ch)
Environmental Physics, EAWAG, CH-8600 Dübendorf, Switzerland

Received: 4 February 2000; Accepted in final form: 27 April 2000

Abstract. Continuous direct records of solar variability are limited to the telescopic era covering approximately the past four centuries. For longer records one has to rely on indirect indices such as cosmogenic radionuclides. Their production rate is modulated by magnetic properties of the solar wind. Using a parameterisation of the solar activity and a Monte Carlo simulation model describing the interaction of the cosmic rays with the atmosphere, the production rate for each cosmogenic nuclide of interest can be calculated as a function of solar activity. Analysis of appropriate well-dated natural archives such as ice cores or tree rings offers the possibility to reconstruct the solar activity over many millennia. However, the interpretation of the cosmogenic nuclide records from these archives is difficult. The measured concentrations contain not only information on solar activity but also on changes in the geomagnetic field intensity and the transport from the atmosphere into the archive where, under ideal conditions, no further processes take place. Comparison of different nuclides (e.g. ^{10}Be and ^{14}C) that are produced in a very similar way but exhibit a completely different geochemical behaviour, allows us to separate production effects from system effects.

The presently available data show cyclic variability ranging from 11-year to millennial time scale periodicities with changing amplitudes, as well as irregularly distributed intervals of very low solar activity (so called minima, e.g. Maunder minimum) lasting typically 100 years.

1. Introduction

Solar variability is an important issue from the solar physics as well as from the terrestrial climate point of view. Solar variability is commonly related to magnetohydrodynamic processes within the convective zone. Most phenomena observed at the solar surface such as sunspots, magnetic network, coronal mass ejections, flares and fluctuations in the amount and the spectral distribution of the emitted radiation are connected in various ways to these processes. At present the theoretical understanding is not yet good enough to model the relationship and the dynamics of these solar variability indices based on physical processes.

The importance of solar variability for the Earth is based on the fact that the Sun is by far the most important source of energy. Geothermal and tidal energy are negligible compared to solar radiation. Therefore, any change in solar radiation or its spectral composition is potentially important for the terrestrial climate (Beer et al., 2000; Mende and Stellmacher, 2000). Terrestrial phenomena related to solar variability are aurorae, the magnetic aa-index and the cosmic ray induced neutron flux in the atmosphere (Beer et al., 1996). All solar indices mentioned so far are based on observations or measurements. Their historical records are therefore lim-

Space Science Reviews **94:** 53–66, 2000.

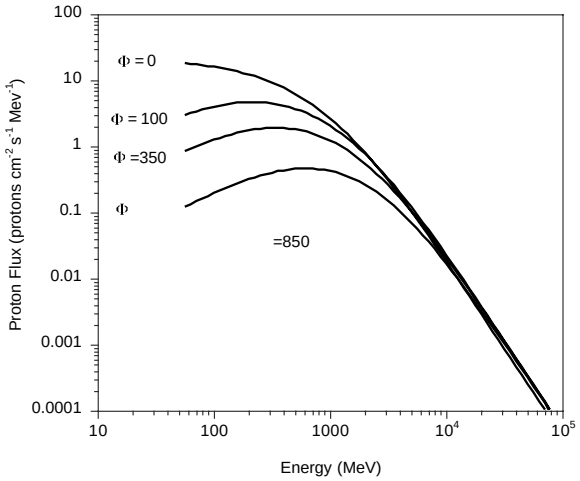

Figure 1. Energy spectrum of the primary cosmic ray proton flux at the top of the atmosphere as a function of the solar modulation parameter Φ. $\Phi = 0$ MeV corresponds to a completely inactive Sun, $\Phi = 850$ MeV to a rather active one.

ited to the period during which observations have been carried out. The longest continuous record is the sunspot record which goes back to the beginning of the 17th century, the time when the telescope was invented. Cosmogenic radionuclides on the other hand offer the unique opportunity to reconstruct solar variability over much longer time scales.

2. Solar Modulation of Cosmogenic Nuclei Production

Cosmogenic nuclei are produced continuously by the interaction of cosmic ray particles with the atmosphere. The primary galactic cosmic rays consist of protons (87%), helium nuclei (12%), and heavier elements (1%). In Fig. 1 the effect of solar modulation on the energy spectrum of primary protons is shown. Modulation of the differential energy spectrum of galactic cosmic rays by solar activity takes place within a radius of about 100 AU around the Sun. During active periods, more coronal mass ejections cause large disturbances in the interplanetary magnetic field, which in turn result in enhanced scatter of galactic cosmic rays away from the inner heliosphere. As a consequence, the net flux reaching the top of the atmosphere is reduced especially at the low energy side of the spectrum. This process has been parameterised using the solar activity parameter Φ. A value of $\Phi = 0$ MeV corresponds to no solar modulation (quiet Sun) and reflects the estimated interstellar spectrum, while $\Phi = 850$ MeV corresponds to a rather active Sun (see Fig. 1).

Using these primary cosmic ray spectra the nuclear interactions with N, O and Ar in the atmosphere can be simulated by Monte Carlo calculations (Masarik and

TABLE I

Some characteristics of three long-lived abundant cosmogenic radionuclides.

Nuclide	Target	Half-life [y]	Production Rate [atoms $cm^{-2}s^{-1}$]	Inventory [tons]
^{14}C	N	5730	2	62
^{10}Be	N, O	1.51×10^6	0.018	105
^{36}Cl	Ar	3.08×10^5	0.0019	8

Beer, 1999). Depending on the original energy, a cascade of secondary particles develops. Mainly the neutrons produced in such cascades generate – by spallation and other nuclear reactions – a variety of new nuclei most of which are stable or very short-lived. Assuming that the interstellar galactic cosmic ray flux is constant in time, the instantaneous production rate of these nuclides at a certain point in the atmosphere depends only on the solar activity and the geomagnetic field intensity. Averaging over the whole atmosphere provides the mean global production rate (Tab. I). Based on those numbers the steady state global amount of each radionuclide is calculated. The production rate of ^{10}Be is significantly lower than that of ^{14}C because it is only produced by high-energy spallation reactions. In the case of ^{36}Cl, the production rate is even lower because it can only be produced from ^{40}Ar which is quite rare (1%) in the atmosphere. We do not make use of ^{36}Cl in this paper. However, since it is sometimes used in literature instead of ^{10}Be we include it in Tab. I.

Two indices that are especially interesting from the climate point of view are the solar diameter (Gilliland, 1981) and the solar irradiance (Lean, 1997; Pap and Fröhlich, 1997). While the first is very difficult to determine with the necessary precision and therefore does not provide conclusive results so far, the latter shows changes over an 11-year Schwabe cycle in the order of 0.1%. To monitor such small changes over decades, extremely stable radiometers are required and careful corrections for degradation processes must be applied. As a consequence, there is no general agreement with regard to the question if there is a trend during the past 2 cycles (Willson, 1997; Beer et al., 2000) or not (Fröhlich and Lean, 1997; Fröhlich, 2000).

The dependence of the production rate of a particular radionuclide on the geomagnetic field intensity and the solar modulation parameter Φ can be calculated using the proton and neutron fluxes obtained from Monte Carlo calculations (Masarik and Beer, 1999). As an example, the results of such calculations are shown in Fig. 2 for ^{10}Be. The geomagnetic field intensity is given in units relative to its present value. The solar modulation parameter Φ varies in the range from 0 MeV (quiet

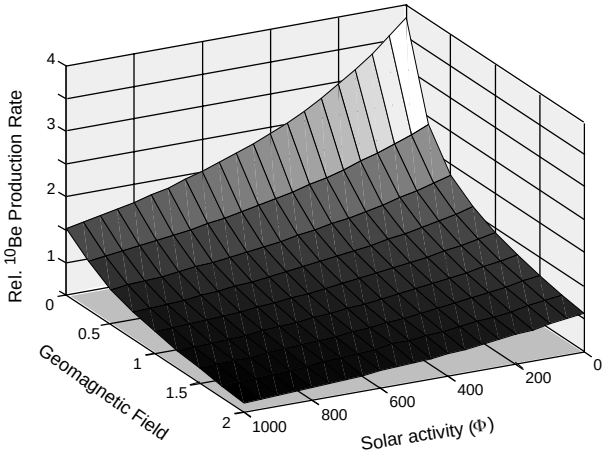

Figure 2. Relative global mean production rate of ^{10}Be as a function of solar activity Φ and geomagnetic field intensity M. M is normalised to the present value. The production rate 1 corresponding to $M = 1$ and $\Phi = 550$ MeV accounts to 0.081 atoms cm^{-2}s^{-1}.

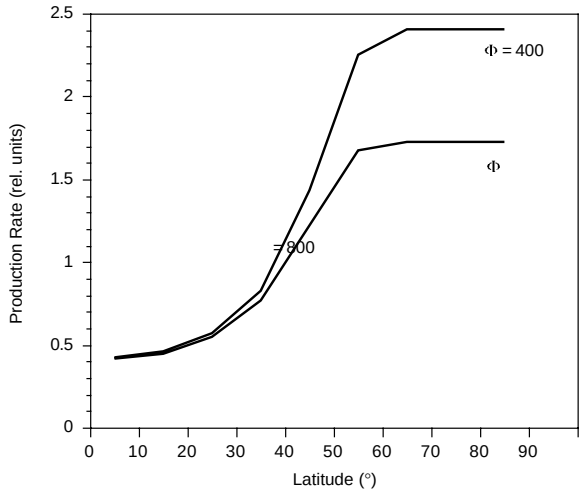

Figure 3. Relative production rate of ^{10}Be as a function of geomagnetic latitude for the present geomagnetic field intensity ($M = 1$) and two different solar activity levels. Note that the solar modulation is effective mainly at high latitudes.

Sun) to 1000 MeV (very active Sun). The relative units of the ^{10}Be production rate are atoms cm^{-2}s^{-1}. For an average $\Phi = 550$ MeV and $M = 1$ the mean global ^{10}Be production rate is 0.018 atoms cm^{-2}s^{-1} (Tab. I).

As a consequence of the geomagnetic dipole field which cuts off low energy cosmic ray particles mainly at low latitudes, the solar modulation effect is strongest in polar regions. Figure 3 shows the effect of the latitude on the amplitude of the ^{10}Be signal assuming that Φ fluctuates between 400 and 800 MeV. For a quantita-

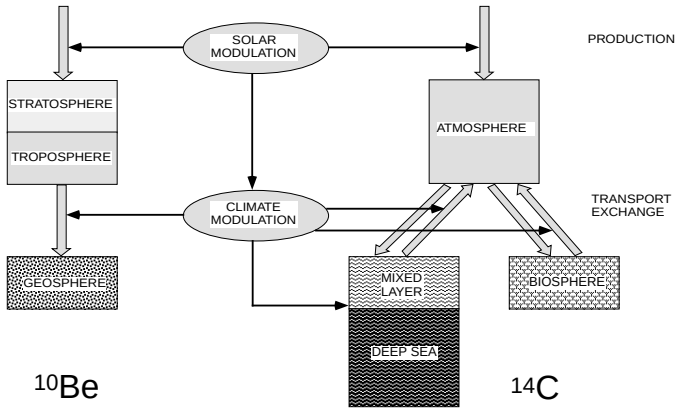

Figure 4. Description of the ^{10}Be and ^{14}C systems by simple box models. Solar modulation affects the production rate of both nuclides in a very similar way. Climate modulation (transport, atmospheric mixing, and deposition), however, leads to completely different effects in the two systems. After its removal from the atmosphere ^{10}Be becomes stored in the geosphere. In contrast ^{14}C continuously exchanges between the different reservoirs resulting in a much more complex behaviour.

tive interpretation of e. g. ^{10}Be in rain or snow it is crucial not only to understand the spatial and temporal variations of the production rate but also the subsequent atmospheric mixing and transport processes. Typical residence times are in the order of years for the stratosphere and weeks for the troposphere. Since about half of the production takes place in the stratosphere, ^{10}Be measurements with a time resolution of less than 1 year mainly reflect atmospheric transport processes. In contrast to the production rate variations that can be modelled quite well, no models based on physico-chemical processes are available today to describe the atmospheric pathways of cosmogenic nuclides from their initial position where they are produced to their final destination where they are deposited. Beside some promising attempts using general circulation models (Brost et al., 1991), most authors rely on rather simple box models which, fortunately, appear to be adequate in many cases when considering cosmogenic nuclide variations on time scales longer than one year (Scheffel et al., 1999).

Figure 4 shows examples of box models generally used to describe the behaviour of ^{10}Be and ^{14}C. In the case of ^{10}Be, the atmosphere is divided into the stratosphere and the troposphere. It is assumed that all the ^{10}Be removed from the troposphere stays in the geosphere and that no recycling takes place. In the case of ^{14}C, $^{14}CO_2$ is formed which exchanges between the four main reservoirs: the atmosphere, the biosphere, the mixed layer, and the deep sea. The shorter the periodicity the more the amplitudes of production variations are attenuated due to the large sizes of these reservoirs. For instance, in the case of the 11-year Schwabe cycle the amplitude of the production rate is damped in the atmospheric ^{14}C concentration by about two orders of magnitude. At the same time, the carbon system

causes a periodicity dependent phase lag between production and atmospheric concentration signal (Siegenthaler et al., 1980). Therefore, a quantitative comparison between ^{14}C and other cosmogenic radionuclides such as ^{10}Be and ^{36}Cl is only feasible if based on an appropriate carbon cycle model.

To reconstruct changes of the production rate in the past we need archives where the produced radionuclides are stored in stratigraphically undisturbed layers. Such archives are e. g. ice sheets, glaciers, and sediments in the case of ^{10}Be, tree rings, sediments, and corals in the case of ^{14}C. These archives are assumed to be closed systems with neither internal transport nor any other processes taking place. These assumptions are not always completely fulfilled. ^{10}Be seems to migrate and to become attached to dust grains on time scales of 10^5 years (Baumgartner et al., 1997). Chlorine can become expelled from ice in the form of HCl or from the sea as methyl chloride (Wagnon et al., 1999). In spite of all these disturbing processes the effects on time scales of millennia are rather modest with the possible exception of chlorine.

3. Results

In the following, we will discuss some existing ^{14}C and ^{10}Be data regarding the long-term solar variability.

3.1. ^{14}C

The potential of ^{14}C as a dating tool for organic material was recognised in the early forties, initiating an extensive study of its geochemical cycle and its production history. It was soon obvious that the atmospheric $^{14}C/^{12}C$ ratio exhibits temporal changes of up to about 10% over the last 10'000 years, but that its spatial changes are small in the order of a few permil (tenths of a percent) (McCormac et al., 1998).

This indicates that the atmosphere is globally well mixed regarding ^{14}C. Figure 5 shows the present $\Delta^{14}C$ record (Stuiver et al., 1998) (the relative deviation in permil of the atmospheric $^{14}C/^{12}C$ ratio from a standard value). The $\Delta^{14}C$ curve is characterised by a long-term trend of about 100‰ superimposed to which there are short-term fluctuations of up to 20‰. The long-term trend is mainly caused by the long-term changes in the production rate, the properties of the carbon cycle and the half-life. It is therefore important to keep in mind that the $\Delta^{14}C$ value at any time is not only determined by the actual production rate but also by the production history during the preceding ca. 2 half-lives and by carbon system effects. The short-term $\Delta^{14}C$ fluctuations are characterised by peaks with a typical duration of about 100 years, the so-called Suess-wiggles.

The period 1510–1950 is shown in detail in Fig. 5 (Stuiver and Braziunas, 1993). Sunspot and aurora data strongly suggest that the wiggles can be attributed to periods of low solar activity. The most pronounced of these periods is the Maunder Minimum from 1645–1715 AD. Similarly, less pronounced periods of low

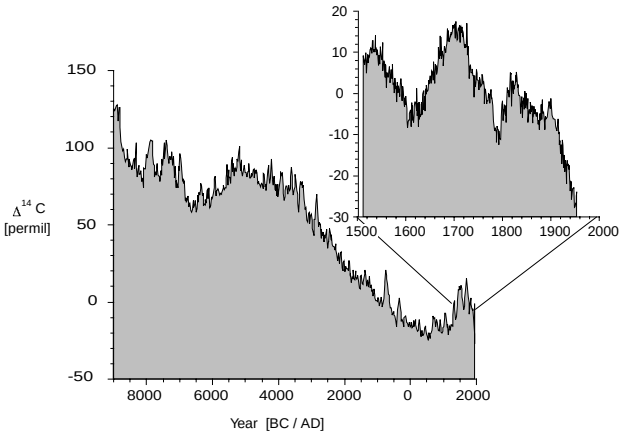

Figure 5. $\Delta^{14}C$ measured in tree rings for the past 11 ky. The record is characterised by short-term variations superimposed to a long-term trend. The short-term variations can be attributed mainly to solar modulation whereas the long-term trend is mainly the result of variations of the geomagnetic field intensity during the past 20 ky and possibly some changes within the carbon system.
The period from 1510 AD to 1950 AD is shown in detail. The peak at 1700 AD corresponds to the maximum of the Maunder minimum, a period famous for its almost complete lack of sunspots. The steep decrease during the 20th century is due to the Suess effect (dilution of the atmospheric ^{14}C content by the growing combustion of fossil fuel) and an increase in solar activity.

solar activity occurred around 1800 (Dalton Minimum) and 1900. The decreasing trend in $\Delta^{14}C$ as from about 1900, however, is to a large extent of anthropogenic origin. The increasing rate of fossil fuel consumption led to an increasing amount of ^{14}C-free CO_2 reducing the $^{14}C/^{12}C$ ratio considerably.

The $\Delta^{14}C$ record covering the past 11500 years (Fig. 5) is based on tree rings. Comparison of the ring width between different trees enabled to match the individual records to a continuous chronology. Before 11500 BP, during the deglaciation, the vegetation was rather different and the number of trees much sparser. Therefore, no continuous record is available yet although several floating chronologies are under construction. Instead of tree rings, other material such as varved sediments (Hajdas, 1993; Hughen et al., 1998; Kitagawa and Van der Plicht, 1998), corals (Bard et al., 1990), or stalagmites have been used. The absolute age can be determined by counting the annual sediment layers or using the U/Th dating technique. However, all these techniques lead to somewhat larger uncertainties in $\Delta^{14}C$ due to dating difficulties or the fact that they do not record directly the atmospheric $\Delta^{14}C$ (corals, stalagmites).

Since solar variability is at least partly quasi-periodic it is interesting to search for periodicities. The most famous periodicity of solar variability is the 11-year Schwabe cycle. Although this periodicity varies considerably between 7 and 18 years since 1750 it seems quite stable and close to 11 years if averaged over longer time periods. Due to the dampening effect of the carbon cycle system, the Schwabe cycle is attenuated strongly and difficult to detect in the $\Delta^{14}C$ (Fig. 5) (Siegenthaler

et al., 1980). In addition, only a small part of the total $\Delta^{14}C$ record has been measured with a time resolution of better than 10 years. A longer periodicity, the existence of which has also been detected in the aurorae records, is the 88-year Gleissberg cycle (Gleissberg, 1965). It is also present in the $\Delta^{14}C$ record, however, its amplitude changes with time (Stuiver and Braziunas, 1993). The most prominent periodicity in the $\Delta^{14}C$ record is the 205-year De Vries cycle. Unfortunately, the observational records are too short to unambiguously attribute this cycle to solar variability. However, the fact that solar minima periods such as Maunder, Spoerer and Wolf occur roughly every 200 years clearly points to a solar origin of this cycle. Its amplitude is also time dependent and its frequency seems stable averaged over long periods of time. Another periodicity often attributed to the Sun is the 2100/2300-year Hallstatt cycle (Damon and Jirikowic, 1992). Although still well in the range of potential solar variability cycles there are no strong arguments yet in favour of a solar origin. Other periodicities found in the power spectrum could be of solar or geomagnetic origin, or related to processes within the carbon cycle system.

3.2. ^{10}BE

^{10}Be can be found in different archives such as ice cores, sediments, and loess (Beer and Sturm, 1995). For studies of solar variability, ice cores are the best-suited archives because they sample the atmospheric ^{10}Be content in the most direct way with a time resolution of one year. One year corresponds to the mean atmospheric residence time and therefore represents the upper limit. The disadvantage of the relatively short atmospheric residence time is, however, that the atmosphere is not necessarily well mixed regarding ^{10}Be and that changes in the removal process from the atmosphere may induce a local component in the ^{10}Be signal measured in an ice core. The fact that ^{36}Cl and ^{10}Be at high latitudes reflect nicely the solar and the geomagnetic modulation of the production rate and the good agreement between these two nuclides with ^{14}C point to a relatively good mixing within the hemispheres. Another difficulty is dating ice cores, especially at greater depth where the annual layer thickness decreases by the thinning effect. On the other hand, ^{10}Be has several advantages compared to ^{14}C. Its production signal is practically not attenuated and is therefore well suited to detect the 11-year Schwabe cycle (Beer et al., 1990). Due to its longer half-life (1.51×10^6 years compared to 5730 years), the time range to investigate is considerably longer (at least 10^5 years). Finally, the ^{10}Be system has no memory effect and therefore stores the actual production rate. In Fig. 6 several ^{10}Be records from Greenland are shown covering different periods with different time resolution. Panel a shows the ^{10}Be concentration from Dye 3 (South Greenland) after applying a low pass filter to remove periodicities shorter than 6 years. The ^{10}Be fluxes in panel b and c have been calculated from the measured ^{10}Be concentration according to the formula

$$F = \rho a c$$

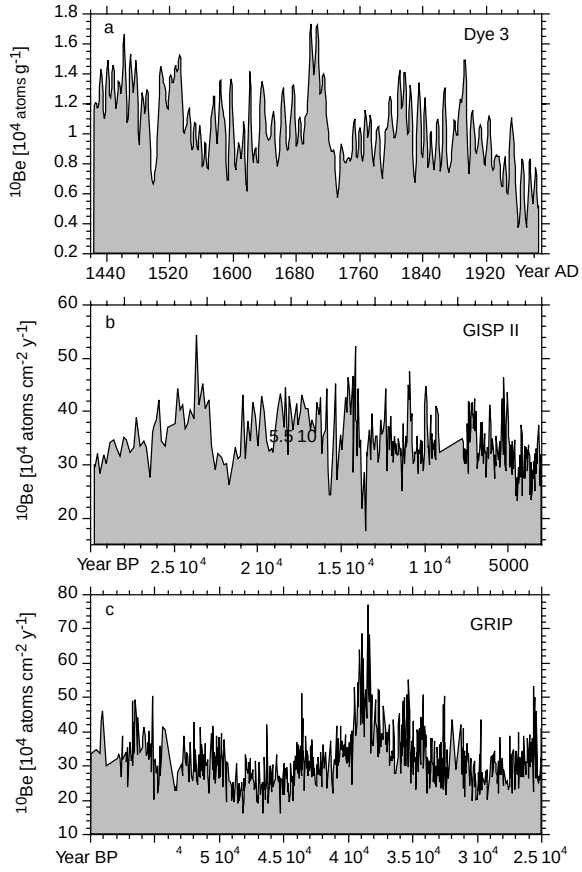

Figure 6. ^{10}Be records with different time resolutions for different time intervals.
a) Annual ^{10}Be concentrations from Dye 3 after removing the short-term fluctuations. b) ^{10}Be flux covering the transition from the last Glaciation into the Holocene . The sharp peaks correspond probably to quiet Sun periods (e.g. Maunder Minimum).
c) ^{10}Be flux during Marine Isotope Stage 3 mainly. The peak close to 40 ky BP and the long-term changes are consistent with changes of the global mean production rate induced by the geomagnetic field intensity.

with the density ρ (g cm^{-3}), the accumulation rate a (cm y^{-1}), and the concentration c (10^4 atoms/g). Since ρ of ice is constant, the flux F is mainly determined by the product of concentration and accumulation rate. During the Holocene the accumulation rate is relatively constant leading to a flux F that looks much the same as the concentration c. During glacial times, however, the accumulation rate changes by up to a factor of 2. As has been shown in earlier studies the ^{10}Be flux can be considered as proportional to the mean global production rate (Wagner et al., 2000a).

As can be seen in Fig. 6 the ^{10}Be records vary on very different time scales. The short-term variations of the ^{10}Be concentration in Fig. 6a reflect the 11-year

Schwabe cycle. Periods of high ^{10}Be concentration correspond to periods of low solar activity such as the Maunder minimum (1645–1715) and partly the Spoerer minimum (before 1540). The general ^{10}Be decrease in the 20th century is mainly due to an increase in solar activity.

Fig. 6b covers the transition from the last glaciation into the Holocene (Finkel and Nishiizumi, 1997). To correct for changes in the accumulation rate at the transition, the ^{10}Be flux has been calculated. The decreasing data density is the consequence of the constant sampling interval and the thinning effect. The narrow peaks most likely correspond to solar minima comparable to the Maunder minimum in panel a.

Fig. 6c shows the ^{10}Be flux of the GRIP ice core between 25 and 65 ky BP (Marine Isotope Stage 3). The main feature is the peak at 38 ky BP that can be attributed to an excursion of the geomagnetic dipole field (so called Laschamp event). The long-term trend can also be explained to a large extent by geomagnetic modulation (Baumgartner et al., 1998). Due to the thinning effect the time resolution given by the sampling interval of 55 cm varies between 30 and 60 years.

A spectral analysis of the ^{10}Be records reveals the following periodicities that can be attributed to solar variability:

TABLE II

Some observed periodicities in the ^{10}Be records of Fig. 6 that can be attributed to solar variability.

Time Interval	Periodicities [y]
1440–1980 AD	10.8, 88
4000–30’000 BP	205
25’000–50’000	205

In the case of ^{10}Be, the most prominent periodicity is the 11-year Schwabe cycle. Its presence has been confirmed for the full length of the Dye 3 annual record back to 1423 AD (Beer et al., 1994). Even during the Maunder minimum when hardly any sunspots could be observed the cycle is still clearly visible in the ^{10}Be data indicating that the solar dynamo was operational during this time (Beer et al., 1998). The Gleissberg cycle was already discovered in the sunspot record (Gleissberg, 1965). Its amplitude changes with time. The 205-year De Vries cycle can also be found with a varying amplitude similar to the case of Δ^{14}C. Recently, it has was found for the first time during the glacial period between 25000 and 50000 BP (Wagner et al., 2000b). This nicely shows the potential of cosmogenic radionuclides to extend our indirect indices of solar variability over much longer time scales. Other periodicities found in these records cannot yet be associated unambiguously with solar variability.

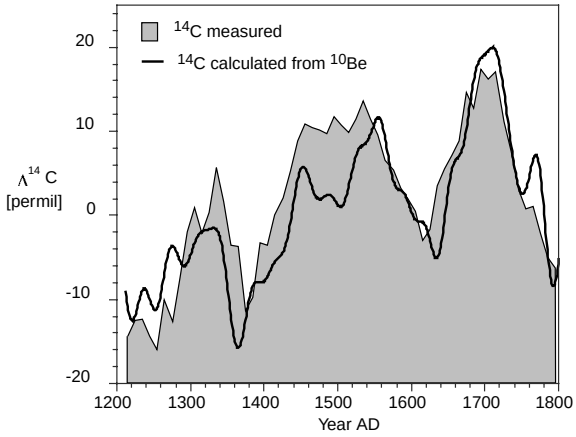

Figure 7. Comparison of the $\Delta^{14}C$ record measured on tree rings with the $\Delta^{14}C$ record calculated based on a combined ^{10}Be record of two ice cores from Milcent (Greenland) and the South Pole. The calculation was performed using the carbon cycle model of Fig. 4 assuming that the combined ^{10}Be record reflects directly the atmospheric production rate. The three periods of low solar activity (Maunder, Spoerer and Wolf) are clearly visible.

4. Comparison ^{14}C-^{10}Be

As discussed earlier, the interpretation of cosmogenic radionuclide records is not straightforward because the signals are composed of a production and a system component (Fig. 4). Since we are interested here in solar variability, we need to separate the production component containing the solar signal from the system component. One solution to this problem is to compare ^{14}C and ^{10}Be. Both nuclides are produced by cosmic ray induced interactions. However, their geochemical behaviour is completely different (see Fig. 4). Therefore the common signal of $\Delta^{14}C$ and ^{10}Be must be attributed to production, the rest to system effects. The comparison can be made in two ways:

1. From the measured atmospheric ^{14}C concentration the production rate is calculated using a carbon cycle model. This calculated production rate is then compared with ^{10}Be data.
2. The ^{10}Be signal is considered as the true production signal and the corresponding atmospheric ^{14}C concentration is calculated based on a carbon cycle model. This calculated data is then compared with the measured ^{14}C record.

We prefer the second approach which has been successfully used already earlier (Beer et al., 1984; Bard et al., 1997). As an example of such a comparison Fig. 7 shows the period 1200 to 1800 AD. The combined ^{10}Be concentration data from Milcent (Greenland) and South pole have been used to calculate the expected $\Delta^{14}C$ record (Beer et al., 1991).

The good agreement with the measured tree ring $\Delta^{14}C$ record clearly indicates that the dominant source of variability in the Holocene is the production rate, most

likely caused by solar modulation. A similar good agreement is obtained for the Holocene periods for which detailed ^{10}Be data from Greenland and Antarctica are available. From this we conclude that the atmosphere seems to be relatively well mixed for ^{10}Be as well and that therefore the local component of the ^{10}Be signal is quite small. Larger differences between measured and calculated Δ^{14}C are to be expected for the last deglaciation when the climate was very unstable. Δ^{14}C is especially sensitive to changes in the deep-water formation. If the global deep-water formation is reduced as postulated e.g. by Broecker et al. (1999) less ^{14}C enters the oceans. This leads to a build-up of ^{14}C and a higher concentration in the atmosphere. Since deep-water formation does not affect the ^{10}Be concentration the calculated and measured Δ^{14}C would be different.

The separation of the production from the system signal still leaves an open problem. Changes in the production rate can be caused either by solar or by geomagnetic modulation. In principle, these two effects could be separated by comparing two records, one from the equator (reflecting magnetic effects) and the other from a polar region (reflecting solar modulation). However, due to the observed good atmospheric mixing such a separation is not feasible. As a general rule, we can assume that short periodicities (< 1 ky) are most likely of solar origin whereas longer periodicities (> 3 ky) are probably caused by magnetic modulation. For a more reliable separation independent information is required, e. g. in the form of paleomagnetism derived from remanence measurements on sediments (Wagner et al., 2000a).

5. Conclusions

A better knowledge of the long-term solar variability is crucial not only for solar physics, but also for environmental physics and climatology. The observational records of direct indices of solar variability such as sunspots are limited to the telescopic era and cover roughly 400 years. Indirect indices such as cosmogenic nuclides have the potential to extend these records significantly to 100'000 years using accurately dated ice cores. The main difficulty in applying cosmogenic nuclides is that they provide a complex signal containing not only information on the production rate, but also on geochemical system effects. By combining different nuclides (e. g. ^{10}Be and ^{14}C), the separation of these effects is possible. Several cycles related to solar variability can be found in the records available today (11-year Schwabe, 88-year Gleissberg, 205-year De Vries). A fundamental issue to address in the future is establishing a relationship between solar variability as derived from cosmogenic nuclides and solar irradiance. This relationship is crucial to distinguish between natural and anthropogenic climate changes. It requires the identification of the physical processes on the Sun that are responsible for long-term changes of solar irradiance. In particular, a basic question is whether solar irradiance changes are only the result of photospheric processes (sunspot blocking, magnetic network)

or whether there are also changes involved in the energy transport through the convective zone.

Acknowledgements

I am indebted to W. Mende, G. Wagner, and R. von Steiger for valuable comments and suggestions. The manuscript was further improved by the help of R. Muscheler, R. Stellmacher and C. Wedema. This work was supported by the Swiss National Science Foundation.

References

Bard, E., Hamelin, B., Fairbanks, R. G., and Zindler, A.: 1990, 'Calibration of the ^{14}C time scale over the past 30,000 years using mass spectrometric U-Th ages from Barbados corals', *Nature* **345**, 405–410.

Bard, E., Raisbeck, G. M., Yiou, F., and Jouzel, J.: 1997, 'Solar modulation of cosmogenic nuclide production over the last millenium: comparison between ^{14}C and ^{10}Be records', *Earth. Planet. Sci. Let.* **150**, 453–462.

Baumgartner, S., Beer, J., Masarik, J., Wagner, G., Meynadier, L., and Synal, H.-A.: 1998, 'Geomagnetic modulation of the ^{36}Cl flux in the GRIP ice core, Greenland', *Science* **279**, 1330–1332.

Baumgartner, S., Beer, J., Wagner, G., Kubik, P. W., Suter, M., Raisbeck, G. M., and Yiou, F.: 1997, '^{10}Be and dust', *Nucl. Instr. Meth.* **B123**, 296–301.

Beer, J., AndrÈe, M., Oeschger, H., Siegenthaler, U., Bonani, G., Hofmann, H., Morenzoni, E., Nessi, M., Suter, M., Wölfli, W., Finkel, R., and Langway Jr., C.: 1984, 'The Camp Century ^{10}Be Record: Implications for Long-Term Variations of the Geomagnetic Dipole Moment', *Nucl. Instrum. Meth.* **B5**, 380–384.

Beer, J., Baumgartner, S., Hannen-Dittrich, B., Hauenstein, J., Kubik, P., Lukasczyk, C., Mende, W., Stellmacher, R., and Suter, M.: 1994, 'Solar Variability Traced by Cosmogenic Isotopes', in *The Sun as a Variable Star: Solar and Stellar Irradiance Variations*, J. M. Pap, C. Fröhlich, H. S. Hudson and S. K. Solanki (eds.), pp. 291-300, Cambridge University Press.

Beer, J., Blinov, A., Bonani, G., Finkel, R. C., Hofmann, H. J., Lehmann, B., Oeschger, H., Sigg, A., Schwander, J., Staffelbach, T., Stauffer, B., Suter, M., and Wölfli, W.: 1990, 'Use of ^{10}Be in polar ice to trace the 11-year cycle of solar activity', *Nature* **347**, 164–166.

Beer, J., Mende, W., R., S., and White, O. R.: 1996, 'Intercomparisons of proxies for past solar variability', in *Climate variations and forcing mechanisms of the last 2000 years*, P. D. Jones, R. S. Bradley and J. Jouzel (eds.), Vol. I41, Springer-Verlag, Heidelberg.

Beer, J., Mende, W., and Stellmacher, R.: 2000, 'The role of Sun in climate forcing', *Quat. Sci. Rev.* **19**, 403–415.

Beer, J., Raisbeck, G. M., and Yiou, F.: 1991, 'Time Variations of ^{10}Be and Solar Activity', in *The Sun in Time*, C. P. Sonett, M. S. Giampapa and M. S. Matthews (eds.), pp. 343-359. Univ. of Arizona press, Tucson.

Beer, J., and Sturm, M.: 1995, 'Dating of lake and loess sediments','*Radiocarbon* **37**, 81–86.

Beer, J., Tobias, S. M., and Weiss, N. O.: 1998, 'An active Sun throughout the Maunder minimum', *Solar Physics* **181**, 237–249.

Broecker, W. S., Sutherland, S., and Peng, T.-H.: 1999, 'A possible 20th-century slowdown of southern ocean deep water formation', *Science* **286**, 1132–1135.

Brost, R. A., Feichter, J., and Heimann, M.: 1991, 'Three-dimensional simulation of ^{7}Be in a global climate model', *J. Geophys. Res.* **96**, 22,423–22,445.

Damon, P. E., and Jirikowic, J. L.: 1992, 'The Sun as a low-frequency harmonic oscillator', *Radiocarbon* **34**, 199–205.

Finkel, R. C. and Nishiizumi, K.: 1997, 'Beryllium-10 concentrations in the Greenland ice sheet project 2 ice core from 3–40 ka', *J. Geophys. Res.* **102**, 26,699–26,706.

Fröhlich, C., and Lean, J.: 1997, 'Total Solar Irradiance Variations', in *IAU Symposium 185*, F. L. Deubner (ed.), Kluwer Academic Publ., Dordrecht.

Fröhlich, C.: 2000, *Space Sci. Rev.*, this volume.

Gilliland, R. L.: 1981, 'Solar radius variations over the past 265 years', *Astrophys. J.* **248**, 1144–1155.

Gleissberg, W.: 1965, 'The eighty-year solar cycle in auroral frequency numbers', *J. Br. Astron. Assoc.* **75**, 227.

Hajdas, I.: 1993, 'Extension of the Radiocarbon Calibration Curve by AMS Dating of Laminated Sediments of Lake Soppensee and Lake Holzmaar', PhD Thesis, ETH Zürich.

Hughen, K., Overpeck, J. T., Lehmann, S., Kashgarian, M., Southon, J., Peterson, L. C., Alley, R., and Sigman, D. M.: 1998, 'Deglacial changes in ocean circulation from an extended radiocarbon calibration', *Nature* **391**, 65–68.

Kitagawa, H., and Van der Plicht, J.: 1998, 'A 40,000-year varve chronology from lake Suigetsu, Japan: Extension of the ^{14}C calibration curve', *Radiocarbon* **40**, 505–515.

Lean, J.: 1997, 'The Sun's variable radiation and its relevance for Earth', *Ann. Rev. Astron. Astrophys.* **35**, 33–67.

Masarik, J., and Beer, J.: 1999, 'Simulation of particle fluxes and cosmogenic nuclide production in the Earth's atmosphere', *J. Geophys. Res.* **104**, 12,099–13,012.

McCormac, F. G., Hogg, A. G., Higham, T. F. G., Lynch-Stieglitz, J., Broecker, W. S., Baillie, M. L. L., Xiong, L., Pilcher, J. R., Brown, D., and Hoper, S. T.: 1998, 'Temporal variation in the interhemispheric ^{14}C offset', *Geophys. Res. Lett.* **25**, 1321–1324.

Mende, W. and Stellmacher, R.: 2000, *Space Sci. Rev.*, this volume.

Pap, J. M., and Fröhlich, C: 1997, 'Total irradiance variations', *J. Atmos. Solar-Terr. Phys.*, 1–13.

Scheffel, C., Blinov, A., Massonet, S., Sachsenhauser, H., Stan-Sion, C., Beer, J., Synal, H. A., Kubik, P. W., Kaba, M., and Nolte, E.: 1999, '^{36}Cl in modern atmospheric precipitation', *J. Geophys. Res.* **26**, 1401–1404.

Siegenthaler, U., Heimann, M., and Oeschger, H.: 1980, '^{14}C Variations Caused by Changes in the Global Carbon Cycle', *Radiocarbon* **22**, 177–191.

Stuiver, M., and Braziunas, T. F.: 1993, 'Sun, Ocean, Climate and Atmospheric $^{14}CO_2$, an evaluation of causal and spectral relationships', *The Holocene* **3**, 289–305.

Stuiver, M., Reimer, P. J., Bard, E., Beck, J. W., Burr, G. S., Hughen, K. A., Kromer, B., McCormac, G., Van der Plicht, J., and Spurk, M.: 1998, 'INTCAL98 Radiocarbon age calibration, 24,000-0 cal BP', *Radiocarbon* **40**, 1041–1083.

Wagner, G., Masarik, J., Beer, J., Baumgartner, S., Imboden, D., Kubik, P. W., Synal, H.-A. and Suter, M.: 2000a, *Nucl. Instr. Meth.*, in press.

Wagner, G., Beer, J., Masarik, J., Muscheler, R., Kubik, P.W., Laj, C., Mende, W., Raisbeck, G. M., and Yiou, F: 2000b, 'Presence of the solar de Vries cycle (205 years) during the last ice age', *Geophys. Res. Lett.*, submitted.

Wagnon, P., Delmas, R. J. and Legrand, M.: 1999, 'Loss of volatile acid species from upper firn layers at Vostok, Antarctica', *J. Geophys. Res.* **104**, 3423–3432.

Willson, R. C.: 1997, 'Total solar irradiance trend during solar cycles 21 and 22', *Science* **277**, 1963–1965.